

ORIGINAL ARTICLE

Zinc(II), palladium(II) and uranyl(II) complexes of  
6-amino-4-hydroxy-2-mercaptopyrimidine

Fatema A.El-Morsy<sup>1</sup>, Ian S.Butler<sup>2</sup>, Shadia El-Sayed<sup>3</sup>, Sahar I.Mostafa<sup>1,\*</sup>

<sup>1</sup>Chemistry Department, Faculty of Science, Mansoura University, Mansoura 35516, (EGYPT)

<sup>2</sup>Department of Chemistry, McGill University, Montreal, QC, Canada H3A 2K6, (CANADA)

<sup>3</sup>Chemistry Department, Faculty of Science, Damietta University, (EGYPT)

E-mail: sihmostafa@yahoo.com

Received: 28<sup>th</sup> September, 2013 ; Accepted: 3<sup>rd</sup> November, 2013

**Abstract** : New complexes of 6-amino-4-hydroxy-2-mercaptopyrimidine (Hahmp), [Zn(ahmp)<sub>2</sub>], [Zn(ahmp)(bpy)]Cl, [Zn(Hahmp)(H<sub>2</sub>O)<sub>2</sub>(SO<sub>4</sub>)], [Pd(bpy)(ahmp)]Cl, [Pd(bpy)(Hahmp)]Cl<sub>2</sub> and *trans*-[UO<sub>2</sub>(ahmp)<sub>2</sub>] have been synthesized and characterized on the basis of elemental analyses, IR, <sup>1</sup>H-NMR, UV-visible and ESI-mass spectroscopy, and thermal and molar conductivity measurements. 6-Amino-4-hydroxy-2-mercaptopyrimidine exhibits two modes of chelation in these complexes as a neutral bidentate ligand through the cyclic nitrogen (N-3) and thione sulfur at-

oms, a mononegative bidentate ligand through the deprotonated cyclic nitrogen (N-1) and thione sulfur atom, or a mononegative bidentate ligand through the cyclic nitrogen (N-3) and deprotonated hydroxy centers. The free Hahmp ligand and some complexes have been tested against the human serous ovarian cancer ascites, OV 90 cell line.

**Keywords** : Hahmp; Zinc; Palladium; Spectra; Complexes; Anticancer.

INTRODUCTION

The pyrimidine ring system occurs widely in living organisms<sup>[1]</sup>. Pyrimidine itself is not found in nature but compounds containing pyrimidinerings systems are well known and are biological active. Pyrimidine is an important component of nucleic acids and is used as a building block in pharmaceutical industries<sup>[2-4]</sup>. 4-Hydroxy-2-mercaptopyrimidine (thiouracil) derivatives are potential therapeutics, i.e., as antiviral and anticancer

agents<sup>[5]</sup>. In addition, pyrimidine derivatives in transition metal complexes are of considerable interest because of their well-known anti-cancer, anti-metastase and anti-microbial activity<sup>[6]</sup>. Over the past few years, our laboratory has been actively involved in the synthesis of various transition metal complexes of 2-thiopyrimidine derivatives<sup>[7-10]</sup> and number of these complexes have been evaluated as anticancer agents against *Ehrlich ascites* tumor cells (EACs)<sup>[13]</sup> and human breast cancer MDA-MB231 cell line<sup>[10]</sup>.

# ORIGINAL ARTICLE

In continuation of our interest in the synthesis of new complexes with expected pharmaceutical activity, we report here the synthesis of complexes of 6-amino-4-hydroxy-2-mercaptopyrimidine with Zn(II), Pd(II) and  $\text{UO}_2^{2+}$ . The structures of the complexes were discussed on the bases of their elemental analyses, spectra (IR, UV-vis., NMR, mass), and thermal and molar conductivity measurements. The anticancer activity of Hahmp and its Pd(II) and Zn(II) complexes have been tested against the human serous ovarian cancer ascites, OV 90 cell line.

## EXPERIMENTAL

### Materials and measurements

All reagents and solvents were purchased from Alfa/Aesar and the manipulations were performed under aerobic conditions using the materials and solvents as received.  $[\text{Pd}(\text{bpy})\text{Cl}_2]^{[11]}$  was prepared by the literature methods indicated.

The human serous ovarian cancer ascites, OV 90 cell line, were obtained from the American Type Culture Collection (ATCC catalog number). Cells were maintained in Dulbecco's Modified Eagle Medium (Wisent Inc., St-Bruno, Canada) supplemented with 10% FBS, 10 mM HEPES, 2 mM L-gutamine and 100  $\mu\text{g}/\text{ml}$  penicillin/streptomycin (GibcoBRL, Gaithersburg, MD). In all assays, cells were plated 24 h before drug treatment.

Infrared spectra were recorded on a Nicolet 6700 Diamond ATR spectrometer in the 4000- 200  $\text{cm}^{-1}$  range. NMR spectra were recorded on VNMRs 200 and 500 MHz spectrometer in  $\text{DMSO}-d_6$  using TMS as reference. Mass spectra (ESI-MS) were recorded using LCQ Duo and double focusing MS25RFA instruments, respectively. Electronic spectra were measured in DMF using a Hewlett-Packard 8453 spectrophotometer. Thermal analyses were made in the 20–800°C range at a heating rate of 20°C  $\text{min}^{-1}$ , using Ni and NiCo as references, on a TA instrument TGA model Q500Analyzer TGA-50. Molar conductivity measurements were carried out at room temperature on a YSI Model 32 conductivity bridge.

### (A) Synthesis

#### (a) $[\text{Zn}(\text{ahmp})_2] \cdot 4/3\text{H}_2\text{O}$

Zinc chloride (0.136 g, 1 mmol) in water (2mL)

was added to Hahmp (0.143 g, 1 mmol) in ethanol containing KOH (0.056 g, 1 mmol; 10mL). The reaction mixture was heated under reflux for 12h, during which an off-white precipitate was obtained. It was filtered off, washed with water, ethanol and air-dried. Yield: 75%. Anal. Calcd. for  $\text{C}_8\text{H}_{10.7}\text{N}_6\text{O}_{3.3}\text{S}_2\text{Zn}$ : C, 25.7; H, 2.9; N, 22.5; S, 17.1; Zn, 17.5 %, Found: C, 25.8, H, 3.0; N, 22.4; S, 17.2; Zn, 17.6%. Conductivity data ( $10^{-3}$  M in DMF):  $\Lambda_M = 4.0 \text{ ohm}^{-1}$ . IR ( $\text{cm}^{-1}$ ) 3442, 3310, 3233, 1545, 1325, 1273, 1153, 553, 490.  $^1\text{H}$  NMR ( $d_6$ -DMSO/TMS, ppm),  $\delta$ : 11.41 (s, 1H, O(4)H); 4.50 (s, 1H, C(5)H); 5.46 (s, 2H,  $\text{NH}_2$ ). ESI-MS:  $m/z$ , 700  $[\text{Zn}(\text{ahmp})_2]^+$ , 414.9  $[\text{Zn}_2(\text{ahmp})]^+$ , 349.3  $[\text{Zn}(\text{ahmp})]^+$ , 207.5  $[\text{Zn}(\text{ahmp})]^+$ .

#### (b) $[\text{Zn}(\text{Hahmp})(\text{H}_2\text{O})_2(\text{SO}_4)]$

Zinc sulfate (0.16 g, 1 mmol) in water (2 mL) was added to Hahmp (0.143 g, 1 mmol) in ethanol (10 mL). The reaction mixture was heated under reflux for 36h, during which a pale yellow precipitate was obtained. This precipitate was filtered off, washed with water, ethanol and air-dried. Yield: 51%. Anal. Calcd. for  $\text{C}_4\text{H}_5\text{N}_3\text{O}_5\text{S}_2\text{Zn}$ : C, 14.1; H, 2.6; N, 12.3; S, 18.8; Zn, 19.2 %, Found: C, 13.9, H, 2.7; N, 12.4; S, 19.2; Zn, 19.4%. Conductivity data ( $10^{-3}$  M in DMF):  $\Lambda_M = 2.0 \text{ ohm}^{-1}$ . IR ( $\text{cm}^{-1}$ ) 3440, 3315, 3223, 1645, 1562, 1400, 1253, 1193, 568, 459.  $^1\text{H}$  NMR ( $d_6$ -DMSO/TMS, ppm),  $\delta$ : 11.53 (s, 1H, O(4)H); 4.54 (s, 1H, C(5)H); 6.16 (s, H, NH); 5.54 (s, 2H,  $\text{NH}_2$ ). ESI-MS:  $m/z$ , 341  $[\text{Zn}(\text{ahmp})(\text{H}_2\text{O})_2(\text{SO}_4)]^+$ , 305.8  $[\text{Zn}(\text{ahmp})(\text{SO}_4)]^+$ , 207.9  $[\text{Zn}(\text{ahmp})]^+$ .

#### (c) $[\text{Zn}(\text{ahmp})(\text{bpy})]\text{Cl}$

$\text{ZnCl}_2$  (0.068 g, 0.5 mmol) in water (2mL) was added to ethanolic solution of Hahmp (0.072 g, 0.5 mmol; 10 mL) and bpy (0.078 g, 0.5 mmol) in ethanol (5mL) was added drop by drop with constant stirring over 75 min. The reaction mixture was heated under reflux for 16h. The yellow precipitate was filtered off, washed with ethanol and air-dried. Yield: 82%. Anal. Calcd. for  $\text{C}_{14}\text{H}_{12}\text{ClN}_5\text{OSZn}$ : C, 42.1; Cl, 8.9; H, 3.0; N, 17.5; S, 8.0; Zn, 16.4%, Found: C, 42.0; Cl, 9.0; H, 3.0; N, 17.4; S, 8.0; Zn, 16.5%. Conductivity data ( $10^{-3}$  M in DMF):  $\Lambda_M = 82.0 \text{ ohm}^{-1}$ . IR ( $\text{cm}^{-1}$ ) 3400, 3313, 3213, 1523, 1408, 1267, 1158, 552, 448.  $^1\text{H}$  NMR ( $d_6$ -DMSO/TMS, ppm)  $\delta$ : 11.64 (s, 1H, O(4)H); 4.64 (s, 1H, C(5)H); 6.21 (s, 2H,

NH<sub>2</sub>). ESI-MS (*m/z*): 364.1 [Zn(ahmp)(bpy)]<sup>+</sup>, 266.9 [Zn(bpy)(ahmp-C<sub>4</sub>H<sub>4</sub>N<sub>2</sub>O)]<sup>+</sup>.

**(d) [Pd(bpy)(Hahmp)]Cl<sub>2</sub>**

[Pd(bpy)Cl<sub>2</sub>] (0.085 g, 0.25 mmol) in methanol-benzene (3:2 v/v, 5 mL) was added to Hahmp (0.036 g, 0.25 mmol) in methanol containing KOH (0.014 g, 0.25 mmol; 10 mL). The reaction mixture was warmed and stirred for 72h. The beige (Pd) or orange (Pt) precipitate was filtered off, washed with methanol and air-dried. Yield: 73%. Anal. Calcd. for C<sub>14</sub>H<sub>13</sub>Cl<sub>2</sub>N<sub>5</sub>OPdS: C, 35.3; Cl, 14.9; H, 2.7; N, 14.7; S, 6.7; Pd, 22.3%. Found: C, 35.5; Cl, 15.0; H, 2.6; N, 14.6; S, 6.7; Pd, 22.3%. Conductivity data (10<sup>-3</sup> M in DMF): Λ<sub>M</sub> = 167.3 ohm<sup>-1</sup>. IR (cm<sup>-1</sup>) 3400, 3312, 3210, 2902, 1637, 1602, 1565, 1374, 1270, 1160, 519, 481. <sup>1</sup>H NMR (d<sub>6</sub>-DMSO/TMS, ppm), δ: 11.92 (s, 1H, OH); 6.17 (s, 1H, N(1)H); 4.55 (s, 1H, C(5)H); 5.57 (s, 2H, NH<sub>2</sub>). ESI-MS (*m/z*): 406[Pd(Hahmp)(bpy)]<sup>+</sup>, 263 [Pd(bpy)]<sup>+</sup>.

**(e) [Pd(bpy)(ahmp)]Cl**

Solid [Pd(bpy)Cl<sub>2</sub>] (0.085 g, 0.25 mmol) was added to Hahmp (0.036 g, 0.25 mmol) in ethanol (10 mL). Et<sub>3</sub>N (0.02 cm<sup>3</sup>, 0.2 mmol) was then added and the reaction mixture was refluxed for 48 h. A brown precipitate was obtained which was filtered off, washed with methanol and air-dried. Yield: 81%. Anal. Calcd. for C<sub>14</sub>H<sub>12</sub>ClN<sub>5</sub>OPdS: C, 38.2; Cl, 8.1; H, 2.7; N, 15.9; S, 7.3; Pd, 24.2%. Found: C, 38.2; Cl, 8.0; H, 2.6; N, 16.0; S, 7.2; Pd, 24.3%. Conductivity data (10<sup>-3</sup> M in DMF): Λ<sub>M</sub> = 88.0 ohm<sup>-1</sup>. IR (cm<sup>-1</sup>) 3402, 3309, 2902, 1637, 1602, 1565, 1380, 1270, 1176, 521, 475. <sup>1</sup>H NMR (d<sub>6</sub>-DMSO/TMS, ppm), δ: 6.16 (s, 1H, N(1)H); 4.59 (s, 1H, C(5)H); 5.55 (s, 2H, NH<sub>2</sub>). ESI-MS (*m/z*): 809.0[Pd(ahmp)(bpy)]<sub>2</sub><sup>+</sup>, 739.1 [Pd<sub>2</sub>(ahmp)(ahmp-C<sub>3</sub>H<sub>4</sub>NO)(bpy)]<sub>2</sub><sup>+</sup>, 442[Pd<sub>2</sub>(ahmp-C<sub>3</sub>H<sub>4</sub>NO)(bpy)]<sup>+</sup>.

**(f) [UO<sub>2</sub>(ahmp)<sub>2</sub>]**

A stirred solution of uranyl nitrate (0.26 g, 0.5 mmol) in MeOH (5 mL) was added to a solution of Hahmp (0.072 g, 0.5 mmol) in MeOH (15 mL). The reaction mixture was stirred and heated under reflux in a steam-bath for 6h, during which an orange precipitate was isolated. It was filtered off, washed with hot MeOH, Et<sub>2</sub>O and air-dried. Yield: 55%.

Anal. Calcd. for C<sub>8</sub>H<sub>8</sub>N<sub>6</sub>O<sub>4</sub>S<sub>2</sub>U: C, 17.3; H, 1.4; N, 15.2; S, 11.6%. Found: C, 17.5, H, 1.3, N, 15.3; S, 11.5%. Conductivity data (10<sup>-3</sup> M in DMF): Λ<sub>M</sub> = 8.0 ohm<sup>-1</sup>. IR (cm<sup>-1</sup>) 3408, 3320, 3237, 1578, 1257, 1190, 972. <sup>1</sup>H NMR (d<sub>6</sub>-DMSO/TMS, ppm), δ: 11.69 (s, 1H, O(4)H), 4.51 (s, 1H, C(5)H); 5.56 (s, 2H, NH<sub>2</sub>). ESI-MS (*m/z*): 555 [UO<sub>2</sub>(ahmp)<sub>2</sub>]<sup>+</sup>, 413[UO<sub>2</sub>(ahmp)]<sup>+</sup>.

**(B) Biological assay**

Growth inhibition assay; ovarian cancer ascites, OV 90 cells were plated at 3000 cells/well in 96-well (100 μL/well) flat-bottomed microliter plates (Costar, Corning, NY). After 24 h incubation, the cells were exposed to different concentrations of each compound continuously for 5 days. Briefly, following drug treatment, the cells were fixed using 50 μL of cold trichloroacetic acid (50%) for 2 h at 4°C, washed with water, stained with sulforhodamine B (SRB 0.4%) overnight at room temperature, rinsed with 1% acetic acid and allowed to dry overnight<sup>[12]</sup>. The resulting colored residue was dissolved in 200 μL Tris base (10 mM, pH 10.0) and optical density was recorded at 490 nm using a microplate reader ELx808 (BioTek Instruments). The results were analyzed by GraphPad Prism (GraphPad Software, Inc., San Diego, CA) and the sigmoidal dose response curve was used to determine 50% cell growth inhibitory concentration (IC<sub>50</sub>). Each point represents the average of two independent experiments performed in triplicate<sup>[12]</sup>.

**RESULTS AND DISCUSSION**

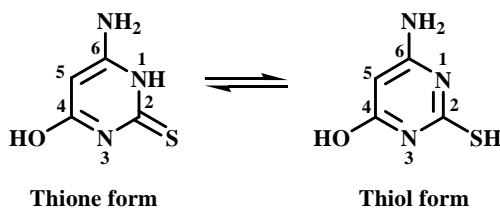
The experimental section describes the synthesis of some new complexes of 6-amino-4-hydroxy-2-mercaptopyrimidine (Hahmp). The elemental analyses of the complexes are in agreement with the assigned formulae. The molar conductivities (Λ<sub>M</sub>) in DMF at room temperature suggest all complexes to be non-electrolytes except for, [M(ahmp)(bpy)]Cl (M = Zn, Pd) which show 1:1 electrolytes while [Pd(Hahmp)(bpy)]Cl<sub>2</sub> is 1:2 electrolyte<sup>[9]</sup>. The complex, [Zn(ahmp)<sub>2</sub>] was prepared from the addition of ZnCl<sub>2</sub> to Hahmp in ethanol under basic conditions while [Zn(Hahmp)(H<sub>2</sub>O)<sub>2</sub>(SO<sub>4</sub>)] was isolated from ZnSO<sub>4</sub> and Hahmp in ethanol. The complex, [Zn(ahmp)(bpy)]Cl, was prepared from ZnCl<sub>2</sub>, Hahmp and 2,2'-bipyridyl in ethanol. The reaction of

# ORIGINAL ARTICLE

Hahmp and  $[\text{Pd}(\text{bpy})\text{Cl}_2]$  in basic methanol-benzene produced  $[\text{Pd}(\text{bpy})(\text{Hahmp})\text{Cl}_2]$  while  $[\text{Pd}(\text{bpy})(\text{ahmp})\text{Cl}]$  produced in presence of  $\text{Et}_3\text{N}$  in ethanol. The reaction of  $\text{UO}_2(\text{NO}_3)_2$  with Hahmp in methanol produced *trans*- $[\text{UO}_2(\text{ahmp})_2]$ .

## Vibrational spectra

The IR spectrum of Hahmp shows bands at 3407 and 3313  $\text{cm}^{-1}$  due to  $\nu_{\text{as}}(\text{NH}_2)$  and  $\nu_{\text{s}}(\text{NH}_2)$  stretching vibrations, respectively, while the strong band at 3215  $\text{cm}^{-1}$  is associated with the  $\nu(\text{OH})$  stretching vibration<sup>[10]</sup>. The absence of the  $\nu(\text{SH})$  mode near 2600  $\text{cm}^{-1}$  and the presence of the  $\nu(\text{NH})$  stretch at 2904  $\text{cm}^{-1}$  and the thioamide bands due to extensive coupling of  $\delta(\text{NH})$ ,  $\nu(\text{C}=\text{N})$ ,  $\nu(\text{NCS})$ , and  $\nu(\text{C}=\text{S})$  modes at 1634, 1585, and (1383, 1271, 1180)  $\text{cm}^{-1}$  support the existence of Hahmp in the thione form (Scheme 1)<sup>[8-10,13,15]</sup>.



**Scheme 1 : Thione-thiol form of 6-amino-4-hydroxy-2-mercaptopyrimidine (Hahmp)**

In complexes,  $[\text{Zn}(\text{Hahmp})(\text{H}_2\text{O})_2(\text{SO}_4)]$  and  $[\text{Pd}(\text{bpy})(\text{Hahmp})\text{Cl}_2]$ , Hahmp functions as a neutral bidentate ligand, coordinating Zn(II) or Pd(II) through the thione sulfur and cyclic nitrogen (N-3) centers, forming four-membered chelate ring. This observation is supported by the shifts in  $\nu(\text{C}=\text{N})$ ,  $\nu(\text{C}=\text{S})$  and  $\nu(\text{N}-\text{C}=\text{S})$  stretches, the slight shift in  $\nu(\text{OH})$  stretch and  $\nu_{\text{as}}(\text{NH}_2)$ ,  $\nu_{\text{s}}(\text{NH}_2)$ ,  $\nu(\text{NH})$  and  $\delta(\text{NH})$  were found more or less in the same positions as in the free ligand<sup>[10]</sup>.

In the complexes,  $[\text{Zn}(\text{ahmp})_2]$  (Figure 1),  $[\text{Zn}(\text{ahmp})(\text{bpy})\text{Cl}]$  and  $[\text{UO}_2(\text{ahmp})_2]$ , Hahmp acts as a mononegative bidentate ligand, coordinating the metal ions through the thione sulfur and the deprotonated cyclic nitrogen (N-1) atoms<sup>[9,10,16]</sup>. This chelation is supported by the shift observed in the  $\nu(\text{C}=\text{S})$  and  $\nu(\text{N}-\text{C}=\text{S})$ , the absence of the  $\nu(\text{NH})$  and  $\delta(\text{NH})$  stretches<sup>[10]</sup>, and  $\nu_{\text{s}}(\text{NH}_2)$ ,  $\nu_{\text{as}}(\text{NH}_2)$ , and  $\nu(\text{OH})$  stretches observed more or less in the same position as in the free ligand<sup>[10,13]</sup>. Also, the same feature has been noted in 6-amino-4-hydroxy-2-thiopyrimidine (Hahtp) complexes,  $[\text{Zn}(\text{ahtp})_2(\text{H}_2\text{O})_2]$ ,  $[\text{Zn}(\text{ahtp})_2(\text{PPh}_3)(\text{H}_2\text{O})]$ ,

$[\text{Ag}(\text{ahtp})(\text{H}_2\text{O})_2]$ ,  $[\text{Ag}(\text{ahtp})(\text{PPh}_3)(\text{H}_2\text{O})]$  and  $[\text{Ag}(\text{ahtp})\text{L}]$  (L = bpy, phen)<sup>[10]</sup>.

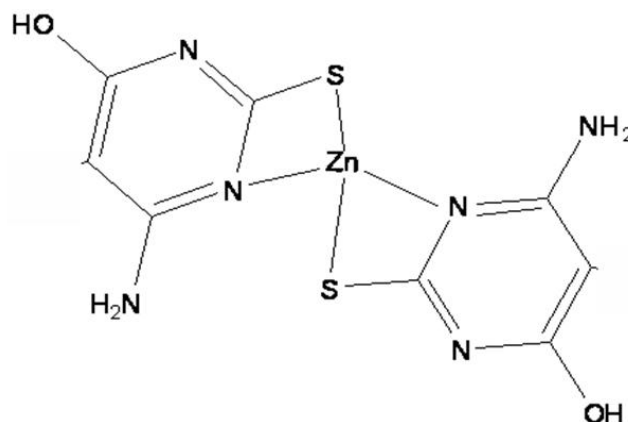


**Figure 1 : Structure of  $[\text{Zn}(\text{ahmp})_2]$**

In the IR spectrum of the complex,  $[\text{Pd}(\text{bpy})(\text{ahmp})\text{Cl}]$ , the  $\nu(\text{OH})$  stretching vibration at 3215  $\text{cm}^{-1}$  in the free ligand is missed, while that arising from  $\nu(\text{C}=\text{N})$  are shifted to lower wavenumbers<sup>[7,8]</sup>. The bands due to the  $\nu_{\text{as}}(\text{NH}_2)$ ,  $\nu_{\text{s}}(\text{NH}_2)$ ,  $\nu(\text{NH})$ ,  $\delta(\text{NH})$ ,  $\nu(\text{NCS})$  and  $\nu(\text{C}=\text{S})$  modes are not affected by complexation, supporting the coordination of the ligand through the deprotonated hydroxy oxygen and cyclic nitrogen (N-3) centers without any participation of the thione sulphur atom as the band near 1180  $\text{cm}^{-1}$  arising from the  $\nu(\text{C}=\text{S})$  stretch remains unchanged<sup>[7-10]</sup>. The IR bands near 854, 841, 750 and 725  $\text{cm}^{-1}$  in  $[\text{M}(\text{ahmp})(\text{bpy})\text{Cl}]$  (M = Zn, Pd) and  $[\text{Pd}(\text{Hahmp})(\text{bpy})\text{Cl}_2]$ , are due to the vibrations of the coordinated bpy<sup>[8]</sup>.

The IR spectrum of *trans*- $[\text{UO}_2(\text{ahmp})_2]$ , exhibits only one U=O stretching band,  $\nu_{\text{as}}(\text{UO}_2)$ , at 972  $\text{cm}^{-1}$  indicating its linear *trans*-dioxo configuration<sup>[8,17]</sup>. The spectra of the complexes show several bands near 500, 420 and 350  $\text{cm}^{-1}$  due to  $\nu(\text{M}-\text{O})$ ,  $\nu(\text{M}-\text{N})$  and  $\nu(\text{M}-\text{S})$  stretches, respectively<sup>[8,18]</sup>. The IR spectrum of  $[\text{Zn}(\text{Hahmp})(\text{H}_2\text{O})_2(\text{SO}_4)]$  shows bands at 1132, 1047, 1053, 989 and 925  $\text{cm}^{-1}$ , indicating the bidentate coordination of  $\text{SO}_4^{2-}$  to Zn(II)<sup>[19]</sup>.

## NMR spectra

The  $^1\text{H-NMR}$  data for the free Hahmp ligand and some of its complexes in  $\text{DMSO-d}_6$  are given in the experimental section. As we have reported earlier, the  $^1\text{H-NMR}$  spectrum of Hahmp shows four singlets at  $\delta$  4.68, 5.66, 6.34 and 11.80 ppm arising from H(5),

NH<sub>2</sub>(6), NH(1) and OH(4), respectively (see Scheme 1 for numbering scheme)<sup>[10]</sup>.

In the <sup>1</sup>H-NMR spectra of the complexes, [Zn(Hahmp)(H<sub>2</sub>O)<sub>2</sub>(SO<sub>4</sub>)] and [Pd(bpy)(Hahmp)Cl<sub>2</sub>], four singlets are observed with upfield shifts for the OH(4) and NH(1) protons indicating the coordination of Hahmp to the metal ions through the thione sulfur and cyclic nitrogen (N-3) atoms<sup>[9,10]</sup>.

In the spectra of the complexes, [Zn(ahmp)<sub>2</sub>], [Zn(ahmp)(bpy)]Cl and *trans*-[UO<sub>2</sub>(ahmp)<sub>2</sub>], the NH(1) singlet is not observed, while that of NH<sub>2</sub> shows an upfield shift confirming the coordination of ahmp through the thione sulfur and deprotonated cyclic (N-1) centers<sup>[10]</sup>.

In the spectrum of the complex, [Pd(bpy)(ahmp)Cl], the hydroxy proton, OH(4), signal is missed while that of H(5) is shifted upfield. This feature supports the coordination of ahmp through the deprotonated hydroxy and cyclic nitrogen (N-3) centers<sup>[7-10]</sup>.

### Electronic spectra

The electronic spectra of the complexes were recorded in DMSO in the 200–800 nm range. The electronic spectra of Hahmp in DMSO show three absorption bands near 210, 250 and 310 nm<sup>[20]</sup>. The electronic spectra of the complexes in DMSO contain intense bands due to ligand-to-metal charge transfer (LMCT) transitions and weaker bands assigned to d–d transitions<sup>[20]</sup>. Transitions below 400 nm are assigned to intra-ligand charge transfer (n→π\* and π→π\*).

The electronic spectra of the diamagnetic [Pd(bpy)(Hahmp)]Cl<sub>2</sub> and [Pd(bpy)(ahmp)]Cl complexes have bands near 475 and 330 nm due to <sup>1</sup>A<sub>1g</sub> → <sup>1</sup>B<sub>1g</sub> and <sup>1</sup>A<sub>1g</sub> → <sup>1</sup>E<sub>1g</sub> transitions in a square-planar configuration<sup>[20,21]</sup>.

### Mass spectra

The mass spectra of the complexes are reported in the Experimental section and their molecular ion peaks are in agreement with their assigned formulae. The mass spectrum of [Zn(ahmp)<sub>2</sub>] shows fragmentation patterns corresponding to the successive degradation of the complex. The first peak at *m/z* 700.0 with 32 % abundance represents the molecular ion [Zn(ahmp)<sub>2</sub>]<sup>+</sup> (Calcd. 699.0). The peaks at 414.9 (Calcd. 415.0), 349.3 (Calcd. 349.5) and 207.5 (Calcd. 207.5) correspond-

ing to [Zn<sub>2</sub>(ahmp)<sub>2</sub>]<sup>+</sup>, [Zn(ahmp)<sub>2</sub>]<sup>+</sup> and [Zn(ahmp)]<sup>+</sup> fragments, respectively<sup>[10]</sup>. The mass spectrum of [Zn(Hahmp)(H<sub>2</sub>O)<sub>2</sub>(SO<sub>4</sub>)] shows a peak at *m/z*, 341 (calcd. 340.5) corresponding to [Zn(Hahmp)(H<sub>2</sub>O)<sub>2</sub>(SO<sub>4</sub>)]<sup>+</sup>. Two peaks at 305.8 (Calcd. 304.5) and 207.9 (Calcd. 208.5) corresponding to [Zn(Hahmp)(SO<sub>4</sub>)]<sup>+</sup> and [Zn(ahmp)]<sup>+</sup>, respectively. The spectrum of [Zn(ahmp)(bpy)]Cl shows a peak at *m/z* 364.1 (Calcd. 363.5) with 78% abundance represents the molecular ion peak [Zn(ahmp)(bpy)]<sup>+</sup>. There is one more peak represents the loss of C<sub>4</sub>H<sub>4</sub>N<sub>2</sub>O fragment at 266.9 (Calcd. 267.9), [Zn(bpy)(ahmp-C<sub>4</sub>H<sub>4</sub>N<sub>2</sub>O)]<sup>+</sup><sup>[10]</sup>. The mass spectra of [Pd(bpy)(Hahmp)]Cl<sub>2</sub> displays signal at *m/z* 406.0 (Calcd. 405.4) with 18.5% abundance, and in agreement with the molecular ion of the complex, [Pd(Hahmp)(bpy)]<sup>+</sup>. The fragmentation patterns indicate the loss of Hahmp and C<sub>4</sub>H<sub>5</sub>N<sub>2</sub>O fragments corresponding to [Pd(bpy)]<sup>+</sup> 263.0 (Calcd. 262.4)<sup>[21]</sup>. The mass spectrum of the [Pd(bpy)(ahmp)]Cl shows the first molecular ion peak at *m/z* 809.0 (Calcd. 808.8) with 32% abundance corresponding to [Pd(ahmp)(bpy)]<sub>2</sub><sup>+</sup>. The peak at 442 (Calcd. 440.8) presents [Pd<sub>2</sub>(ahmp-C<sub>3</sub>H<sub>4</sub>NO)(bpy)]<sup>+</sup> fragment.

### Thermal measurements

The thermal stability and degradation behaviour of [Zn(Hahmp)<sub>2</sub>].4/3H<sub>2</sub>O, [Zn(ahmp)(bpy)]Cl, [Pd(bpy)(ahmp)]Cl<sub>2</sub> and [Pd(bpy)(Hahmp)]Cl, were studied using the thermogravimetric (TG) technique. The weight loss observed below 130°C is due to dehydration as the colours changed from pale to deeper<sup>[22]</sup>.

The thermogram of [Zn(ahmp)<sub>2</sub>].4/3H<sub>2</sub>O shows five TG inflections in the 32 – 154, 155 – 260, 261 – 400, 401 – 507 and 508 – 800°C regions. These weight losses are arising from the release of hydrate water (Calcd. 6.4, Found 6.7%), H<sub>2</sub> and ¼ N<sub>2</sub> (Calcd. 2.4, Found 2.3%), C<sub>3</sub>HNO (Calcd. 17.9, Found 18.2%), NCSN (Calcd. 19.3, Found 19.5%), C<sub>3</sub>H<sub>3</sub>N<sub>2</sub> (Calcd. 17.9, Found 18.0%) fragments, respectively, leaving residue of ZnO (21.8%).

The thermogram of [Zn(ahmp)(bpy)]Cl, is characterized by four weight losses in the 180–285, 286–444, 445–600 and 601–885°C regions. These weight losses are due to the elimination of ½ Cl<sub>2</sub> (Calcd. 8.9, Found 9.1%)<sup>[10]</sup>, C<sub>3</sub>H<sub>4</sub>N<sub>2</sub> (Calcd. 17.0, Found 16.8%), CNS (Calcd. 14.5, Found 14.3%) and 1/2 bpy (Calcd. 19.5,

# ORIGINAL ARTICLE

Found 19.7%) fragments, respectively, leaving ZnO at 775°C (21.8%).

The thermogram of [Pd(bpy)(Hahmp)]Cl<sub>2</sub>, shows two TG inflections in the 145–355 and 356–695°C regions. These weight losses may arise from the release of Cl<sub>2</sub>, C<sub>3</sub>H<sub>5</sub>N<sub>2</sub> (Calcd. 29.4, found 29.6) and bpy, CN (Calcd. 38.2, Found 38.1%) fragments, respectively<sup>[20,21]</sup>, leaving a residue of palladium oxide and azide (25.7%). The thermogram of [Pd(bpy)(ahmp)]Cl shows the first endothermic weight loss step between 100 and 337°C, corresponding to the release of ½ Cl<sub>2</sub> (Calcd. 8.1, Found 8.4%). The decomposition step between 338 and 455°C, is due to the loss of C<sub>4</sub>H<sub>3</sub>N<sub>2</sub>S fragment (Calcd. 22.5, Found 22.7%). The TG inflection between 456 and 608°C is attributed to the loss of ½ bpy and ½ N<sub>2</sub> fragments (Calcd. 20.9, Found 21.1%), leaving PdO and carbide residue representing (28.9%). In some reported transition metal complexes, the thermal decomposition residue is mainly metal or metal oxide, but in the presence of non-stoichiometric oxide, unburned carbon or nitrogen is observed<sup>[10,23]</sup>.

## Anti-cancer activity

Cis-platin is considered to be one of the best known small metal-containing drug molecules. It acts as anti-cancer agent for several human cancers, particularly, testicular and ovarian cancers<sup>[10]</sup>. The side effects, especially nephrotoxicity, limit its widespread use in high doses<sup>[24]</sup>. Thus, the develop new complexes with reduced nephrotoxicity and higher activity has stimulated the synthesis of many new complexes. We have been recently examined the *in vitro* anticancer activity of *DL*-piperidine-2-carboxylic acid (*DL*-H<sub>2</sub>pa) and its complexes, *trans*-[Zn<sub>2</sub>(μ-Ca)<sub>2</sub>(Hpa)<sub>2</sub>Cl<sub>6</sub>], [Pd(bpy)(Hpa)]Cl and [M(pa)(PPh<sub>3</sub>)<sub>2</sub>] against serous ovarian cancer ascites, OV 90 cell line<sup>[25]</sup>.

The ultimate goal of our current research is to develop new complexes with high efficacy against cancer cells. The *in vitro* anticancer activity of the free Hahmp and its complexes, [Zn(Hahmp)<sub>2</sub>], [Zn(bpy)(ahmp)]Cl, [Pd(bpy)(ahmp)]Cl and [Pd(Hahmp)(bpy)]Cl<sub>2</sub> were tested against the serous ovarian cancer ascites, OV 90 cell line in comparison to *cis*-platin as a reference

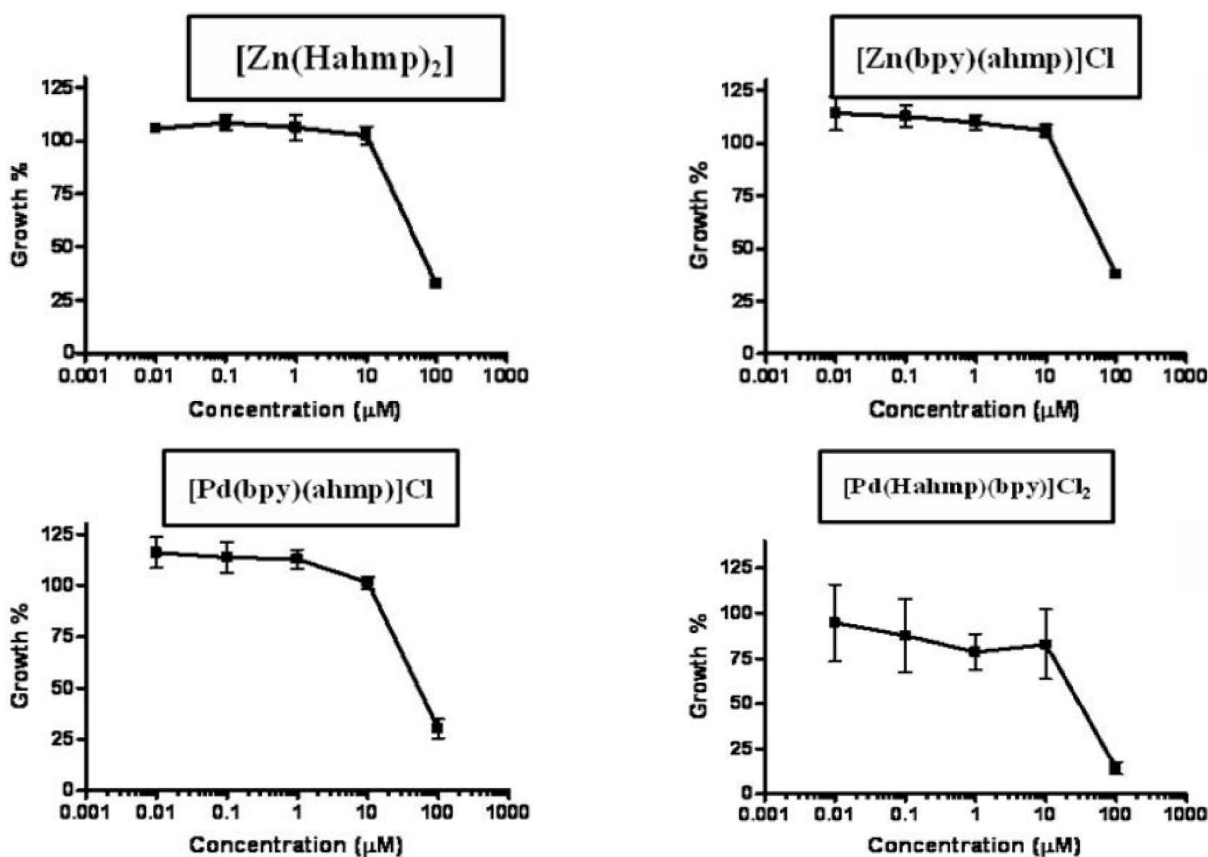


Figure 2 : IC<sub>50</sub> values of [Zn(Hahmp)<sub>2</sub>], [Zn(bpy)(ahmp)]Cl, [Pd(bpy)(ahmp)]Cl and [Pd(Hahmp)(bpy)]Cl<sub>2</sub> tested against the serous ovarian cancer ascites, OV 90 cell line

( $IC_{50} = 31.60$ ). The free Hahmp and its complexes exhibit growth inhibitor activity with mean  $IC_{50}$  values of >100.00, 57.32, 52.41, 43.00 and 32.90, respectively (Figure 2).

Generally, it is accepted that binding of *cis*-platin to genomic DNA (gDNA) in the cell nucleus is the main event responsible for its antitumor properties<sup>[26]</sup>. The damage induced upon binding of cisplatin to gDNA may inhibit transcription, and/or DNA replication mechanisms. Subsequently, these alterations in DNA processing would trigger cytotoxic processes that lead to cancer cell death.

It was reported that, in Pt(II) complexes, the kinetic *trans* effect is responsible for ligand exchange reactions; i.e., donor atoms located *trans* to other donors with strong *trans* effect are more rapidly substituted than ligands in *cis*-positions<sup>[27]</sup>. These features explain the expected activity of mixed Hahmp-bpy complexes [Pd(ahmp)(bpy)]Cl and [Pd(Hahmp)(bpy)]Cl<sub>2</sub>, which attributed to their square-planar geometry as well as the nature and (*cis*-bpy donation)<sup>[9,21,25]</sup>. The anti-cancer activity is increasing since the conductivity and solubility increase<sup>[9]</sup>, this feature explain the activity of [Pd(Hahmp)(bpy)]Cl<sub>2</sub> in comparison to [Pd(ahmp)(bpy)]Cl. On the other hand, the low activity of the complexes, [Zn(ahmp)<sub>2</sub>] and [Zn(bpy)(ahmp)]Cl may be due to the poor solubility and difficulty in hydrolysis to produce their cationic form (in case of [Zn(ahmp)<sub>2</sub>]) or fast interaction with DNA under physiological conditions as well as the tetrahedral geometry of [Zn(bpy)(ahmp)]Cl<sup>[28]</sup>.

## CONCLUSIONS

New complexes of Hahmp have been prepared and characterized. The Hahmp ligand shows three coordination modes are mononegative bidentate, through thione sulfur and deprotonated cyclic nitrogen (N-1) centers or deprotonated hydroxy oxygen and cyclic nitrogen (N-3) centers, and neutral bidentate thione sulfur and cyclic nitrogen (N-3) centers. The free Hahmp and its complexes, [Zn(ahmp)<sub>2</sub>], [Zn(bpy)(ahmp)]Cl, [Pd(Hahmp)(bpy)]Cl<sub>2</sub> and [Pd(ahmp)(bpy)]Cl were tested against the human serous ovarian cancer ascites, OV 90 cell line.

## ACKNOWLEDGEMENTS

We are grateful to a NSERC (Canada) Discovery grant (ISB) for the financial support of this work.

## REFERENCES

- [1] G.Michael; P.Prog.Heterocycle Chem., 231-254 (1996).
- [2] K.K.Ogilvie, R.G.Hamilton, M.F.Gillen, B.K.Radatus, K.O.Smith, K.S.Galloway; Can.J. Chem., **62**, 16 (1984).
- [3] N.Zenker; Thyroid function and thyroid drugs. in: W.O.Foye (Ed); Principles of Medicinal Chemistry, Third Edition. Lea &Febiger, Philadelphia, London, 603 (1990).
- [4] M.B.Deshmukh, S.M.Salunkhe, D.R.Patil, P.V.Anbhule; Eur.J.Med.Chem., **44**, 2651 (2009).
- [5] B.Lippert; Alteration of nucleobasepKa values upon metal coordination, Origin and consequences in, K.D.Karlin (Ed); Prog.Inorg.Chem., Chapter 6, **54**, (2005).
- [6] K.Karidi, A.Garoufis, N.Hadjiliadis, M.Lutz, A.Spek, J.Reedijk; Inorg.Chem., **45**, 10282 (2006).
- [7] S.I.Mostafa, N.Hadjiliadis; Transition Met.Chem., **33**, 529 (2008).
- [8] S.I.Mostafa, C.Papatriantafyllopoulou, S.Perlepes, N.Hadjiliadis; Bioinorg.Chem.Appl.
- [9] S.I.Mostafa, F.A.Badria; Metal-Based Drugs.
- [10] S.El-Sayed, B.Jean Claude, I.Butler, S.Mostafa; J.Mol.Struct., **1028**, 208 (2012).
- [11] (a) W.P.Griffith, S.I.Mostafa; Polyhedron, **11**, 871 (1992); (b) R.I.Kureshy, N.H.Khan, S.H.Abdi, P.Tyer; J.Mol.Cat.A, **121**, 25 (1997); (c) T.A.Stephenson, G.Wilkinson; J.Inorg.Nucl.Chem., **28**, 945 (1966).
- [12] P.Skehan, R.Storeng, D.Scudiero; J.Natl.Cancer Inst., **82**, 1107 (1990).
- [13] (a) G.Tamasi, S.Defazio, L.Chiasserini, A.Sega, R.Cini; Inorg.Chim.Acta, **362**, 1011 (2009); (b) M.D.Gutierrez, R.Lopez, M.A.Romero, J.M.Salas; Canad.J.Chem., **66**, 249 (1988).
- [14] E.L.Torres, M.A.Mendiola; Polyhedron, **24**, 1435 (2005).
- [15] G.Glilub, H.Cohen, P.Paoletti, A.Bencini, D.Meyerstein; J.Chem.Soc., Dalton Trans., **10**, 2055 (1996).
- [16] F.Shaheen, A.Badashah, M.Gielen, L.Marchio, D.deVos, M.K.Khosa; Appl.Organometall.Chem., **21**, 626 (2007).

**ORIGINAL ARTICLE**

---

---

- [17] K.Nakamoto; Infrared and Raman Spectra of Inorganic and Coordination Compounds, John Wiley & Sons, New York, NY, USA, 4th Edition, (1986).
- [18] S.I.Mostafa, K.M.Ibrahim, Z.A.Younis; Inorg. Chem.Ind.J., **2**, 68 (2007).
- [19] V.Ivanovski, V.M.Petrusevski, B.Soptrajanov; J.Mol.Struct., **480-481**, 689-693 (1999).
- [20] S.I.Mostafa; J.Coord.Chem., **61**, 1553 (2008).
- [21] S.I.Mostafa; Transition Met.Chem., **32**, 769 (2007).
- [22] N.A.Anaan, E.M.Saad, S.M.Hassan, I.S.Butler, S.I.Mostafa; Carbohydrate Res., **346**, 775 (2011).
- [23] I.Gabr, H.El-Asmy, M.Emmam, S.I.Mostafa; Transition Met.Chem., **34**, 409 (2009).
- [24] F.P.T.Harmers, W.H.Gispen, J.P.Neijs; Eur.J.Cancer, **27**, 372 (1991).
- [25] A.A.Alie El-Deen, A.E.El-Askalany, R.Halaoui, B.J.Jean-Claude, I.S.Butler, S.I.Mostafa; J.Mol.Struct., **1036**, 161-167 (2013).
- [26] V.Cepeda, M.A.Fuertes, J.Castilla, C.Alonso, C.Quevedo, J.M.Pérez; Anti-Cancer Agents in Medicinal Chemistry, **7**, 3 (2007).
- [27] H.Arzoumanian, G.Agrifoglio, M.V.Capparelli, R.Atencio, A.Briceño, A.Alvarez-Larena; Inorg.Chim.Acta, **359**, 81-89 (2006).
- [28] I.Kostova; Recent Patents on Anti-cancer Drug Discovery, **1**, 1 (2006).